

## Recent Advancement in Photonic Crystal Fiber Based Sensors: A Review

Sandhir Kumar Singh<sup>a\*</sup>, Syed Sadique Anwer Askari<sup>b</sup> & Zeba Akhter<sup>a</sup>

<sup>a</sup>Department of Physics, IIIT Ranchi, Jharkhand 835 217, India

<sup>b</sup>Department of Electronics and Communication Engineering, IIIT Ranchi, Jharkhand 835 217, India

*Received 10 May 2024; accepted 10 October 2024*

This review paper summarizes properties, uses, working principle and applications of the Photonic Crystal Fiber and its comparison with conventional fiber. In simple terms, conventional optical fiber is a wired transmission medium that offers an optical channel that is more reliable as well as flexible than the atmosphere. The most crucial aspects of any communication systems are its bandwidth and signal-to-noise ratio, which determine the channel's capacity. At 1550 nm, the optical fiber link currently has a loss of 0.2 dB/km. A single fiber-optic communication link has a bandwidth of about 50 THz. Thus, the foundation of modern communication systems is made up of fiber optic communication systems. Optical fiber is used in a wide range of sensor applications in addition to communication. However, optical fiber is not able to offer design flexibility. Thus, Photonic Crystal Fiber—a desirable substitute fiber—came into existence. With only little changes to its geometrical dimensions, photonic crystal fiber offers exceptional design freedom and opens opportunities in various sensing applications. This article covers comparative analysis of different sensing parameters like birefringence, confinement loss for liquids mediums like water, ethanol, benzene, glucose solution, human mucosa etc. The geometrical structural dependence of sensitivity of PCF based sensors have been reviewed. Further, for different gases their absorption wavelengths, relative sensitivity, confinement loss at different operating frequencies sensitivity and effective mode area have been reviewed. Performance parameters of PCF-based temperature sensors for different PCF designs have also been analysed. It is suggested that by adjusting the geometrical structure of air holes the performance of PCF based sensors can be optimized.

**Keywords:** Photonic Crystal Fiber(PCF); Refractive index (RI); Dispersion; Chromatic Dispersion; Birefringence; Confinement loss; Nonlinearity; Effective mode Area; Total internal reflection (TIR)

### 1 Introduction

The foundation of modern communication systems is made up of fiber optic communication systems<sup>1,2</sup>. Optical fiber is used in a wide range of sensor applications in addition to communication. However, optical fiber is not able to offer flexible design. Thus, Photonic Crystal Fiber—a desirable substitute fiber—was developed. With only little changes to its geometrical dimensions, PCF provides excellent flexibility in design.

Until now, an optical fiber consisted of a solid wire enclosed in a lower refractive index material. Currently, photonic crystal fibers (PCFs) are recognized as a substitute for conventional fiber technology. PCFs are optical fibers having a periodic arrangement of low-index material in a background of bigger refractive index. They were first exhibited in 1995. PCFs typically consist of undoped silica for the background material and air-holes that spread the length of the fiber to produce the low-index region.

PCFs fall into two primary categories: photonic bandgap and high-index guiding fibers. Because light is contained in a solid core by utilizing the modified total internal reflection process, PCFs in the first category are more akin to traditional optical fibers. The photonic crystal cladding and the core region really have different refractive indices, with the latter having a lower average due to the existence of air holes. The guiding mechanism is called as "modified" because, unlike conventional optical fibers, it's R.I. varies significantly with wavelength rather than remaining constant.

This property offers several new intriguing properties, in conjunction with the significant refractive index difference between silica and air. Furthermore, one of the unique qualities of PCFs is their great degree of design flexibility. Specifically, PCFs with diametrically opposite properties can be obtained by varying the geometric parameters (*i.e.*, dimension or position) of the air-holes in the fiber cross-section. For example, PCFs with a large air-hole fraction in the transverse section and a small silica core have better nonlinear properties than

\*Corresponding author:  
(E-mail: sksingh@iiitranchi.ac.in)

conventional optical fibers, making them suitable for a variety of applications such as supercontinuum generation. On the other hand, fibers can be made with large hole-to-hole spacing and tiny air holes in order to obtain a large modal area, useful for high-power delivery. In contrast to ordinary fibers, PCFs with the right geometric properties can be endlessly single mode, implying that irrespective of the wavelength, only the fundamental mode is guided. Furthermore, a significant asymmetry can be easily added to the PCF core, resulting in fibers with extremely high birefringence levels. Furthermore, there is great freedom in adjusting the PCF dispersion parameters. For example, the zero-dispersion wavelength can be moved into the visible region, and ultra-flattened or strongly negative-sloped dispersion curves can be produced.

A different method than total internal reflection guides light when the PCF core region's refractive index is lower than that of the surrounding photonic crystal cladding. This is achieved by taking use of the photonic bandgap (PBG). Actually, the two-dimensional photonic crystal that makes up the PCF cladding is an air-hole microstructure. Photonic crystals are materials with periodic dielectric characteristics that are distinguished by a photonic bandgap, which prevents light from propagating in specific wavelength ranges.

The PBG effect is also present in nature, as seen by the vivid and lovely colours found in butterfly wings, for instance. By adding a defect, such as an additional or larger air-hole, to the photonic crystal structure, PCFs with a low index core are produced. The PBG prevents light from propagating in the micro structured cladding region, which confines light. This guiding mechanism presents an entirely new range of intriguing possibilities and is not achievable with conventional optical fibers. Specifically, light can be guided in air in PCFs with a hollow core, offering a wide range of prospective applications without the risk of damaging fibers, including high-power delivery and low-loss guidance. Furthermore, air-guiding PCFs exhibit severe dispersion qualities, with the waveguide component heavily predominating, and are nearly insensitive to bending, even for small bending diameter values. Lastly, hollow core PCFs can be effectively used in sensor applications or for nonlinear optics when filled with the appropriate gases or liquids.

Due to its small size and real-time detection of biochemical material in diverse liquids Photonic

crystal fiber (PCF) based refractive index (RI) sensors have been extensively explored and implemented by researchers in recent years. Much work has gone into adapting and exploring ways to optimize different surface plasmon resonance (SPR) based PCF sensors shown in Fig. 1. SPR is one of the important technologies that can be used for a variety of sensory phenomena. It is an optical phenomenon that arises when transverse magnetic (TM) waves or p-polarized waves, under specific circumstances, propagate along the metal-dielectric interface and optically excite surface plasmon waves (SPWs)<sup>4</sup>. The refractive index fluctuation of the liquid adjacent to the metal surfaces greatly affects SPR. Because of this, it may be highly applicable to different sensing methods for the detection of biomolecules and biochemicals both in-situ and at the level of free molecules<sup>5</sup>. Since PCFs offer significant advantages over standard optical fibers in terms of their flexible geometric design, controlled birefringence, and high confinement, their combination with SPR phenomena has attracted the interest of research groups<sup>6</sup>. Different SPR-based PCF sensors have been reported in recent decades. For example, Liu *et al.* presented an SPR-based PCF RI sensor, which uses gold as a plasmonic material and has a claimed sensitivity of 5,500 nm/RIU for analyte RI ranges of 1.23-1.297. A SPR-based PCF biosensor with a gold layer outside the PCF structure, shown in Fig. 2, was proposed by Hasan *et al.* in 20178. The authors found that the highest observed was 2,200 nm/RIU for an analyte range of 1.33–1.36.

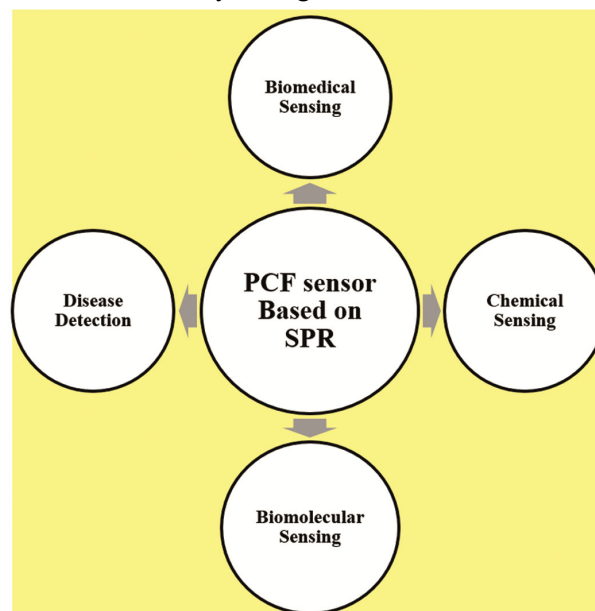


Fig. 1 — Cross section of the PCF-SPR biosensor<sup>3</sup>

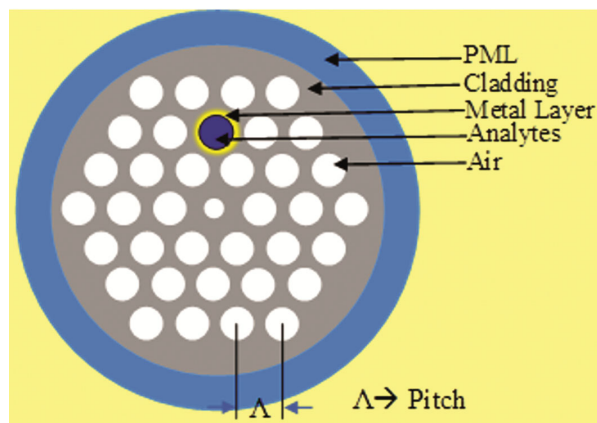


Fig. 2 — Cross section of the PCF-SPR biosensor<sup>3</sup>

## 2 From Conventional Optical Fibers to PCFS

Optical fibers are one of the greatest technological achievements of the 20th century. They carry information in the form of short light pulses over long distances at very fast speeds. From the first low-loss single-mode waveguides in 1970 to being essential parts of the complex international telecommunication network, this technology has advanced at an incredible pace. Optical fibers find several non-telecom uses, such as in sensing, machining and diagnostics, medical beam delivery, and many more areas. Group velocity dispersion, optical losses, optical nonlinearity, and polarization effects are all carefully balanced in modern optical fibers. The system's capabilities and manufacturing technique have been refined almost to their limit after thirty years of intensive development.

Since the 1980s, scientists and engineers have been drawn to various labs by the prospect of structuring materials at the optical wavelength scale, fractions of micrometers or less—in order to create novel optical media, or photonic crystals. The material's regular morphological microstructure, which drastically changes the material's optical characteristics, is essential to the formation of photonic crystals<sup>9</sup>.

They signify the expansion of semiconductor-related results into the field of optics. Actually, the interactions between electrons and the periodic potential variations produced by the crystal lattice determine the band structure of semiconductors. Electron energy levels divided by forbidden bands are derived by solving Schrodinger's wave equation given a periodic potential. PBGs can be generated in photonic crystals, where the Schrodinger equation is replaced by the classical wave equation for the magnetic field, and periodic fluctuations in the

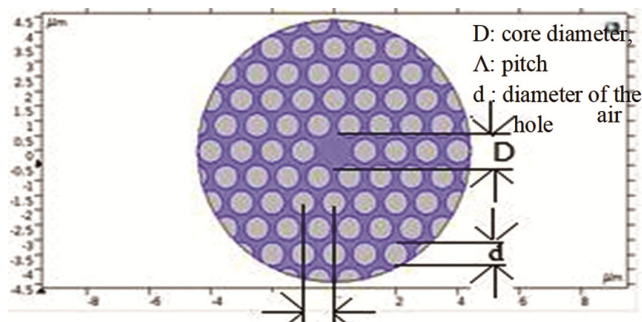


Fig. 3 — Solid Photonic Crystal fiber<sup>12</sup>

dielectric constant, or refractive index, substitute variations in electric potential<sup>10</sup>.

## 3 Types of Photonic Crystal Fibers

A structure consisting of a core and clad that maintains the same propagation law of total internal reflection as a conventional fiber can be used to describe a photonic crystal fiber (PCF). Just as this ionic lattice influences electrons in solids, periodic nanostructures influence photon mobility. It occurs naturally in the shape of colouring the structure<sup>11</sup>.

This unique fiber's core is composed entirely of silica, which can be either solid or hollow. The fiber is referred to as "holey" or "micro structured" because of the air holes that encircle the core and allow light to be limited and transported through the core, which functions as a cavity. It usually consists of two types,

- Index guiding or solid core PCF
- Photonic band gap guiding or hollow core PCF

### 3.1 Indexguiding or solid core PCF

In index guiding PCF light is guided by the principle of modified total internal reflection between the core and cladding. The cladding refractive index in PCF is not constant but it varies with wavelength which is constant in case of conventional fiber. The background material in solid core fiber is commonly silica and the cladding is ordinarily of air holes running along their complete length. Pure silica background with a refractive index of 1.462 and cladding of air holes having refractive index of (1.000) is shown in the Fig. 3. Since silica and air hole have very high refractive index difference, light is guided by TIR which depends on wavelength. The stage delay per unit length in PCF relative to stage delay in vacuum is essentially measured by the Effective Refractive Index.

In Fig. 3, a solid core PCF of core diameter 'D', separation between the consecutive air holes (pitch) 'Δ' and air hole diameter 'd' is shown<sup>11</sup>.

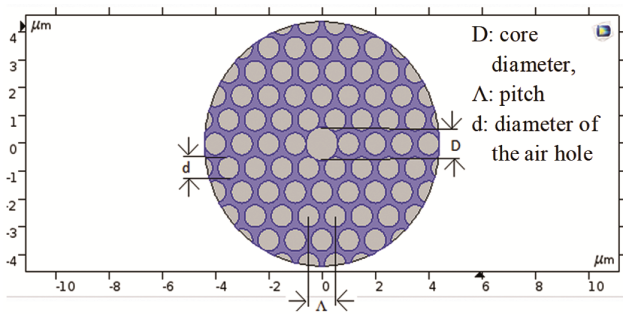


Fig. 4 — Photonic band-gap fiber with hollow cavity in the center<sup>12</sup>

### 3.2 Photonic band-gap guiding or hollow core PCF

In Photonic band-gap fiber the core region of the air holes array is simply changed by a much bigger hole in comparison to the surrounding holes to create a defect. By adding a defect, such as an additional or larger air-hole, to the photonic crystal structure, PCFs with a low index core are produced. Because of the deformity of the structure by introducing bigger air holes the periodicity of the structure is broken, this results in changed optical properties of the fiber. No electromagnetic modes are permitted to pass through the cladding holes. The PBG prevents light from propagating in the microstructure cladding region, which confines light. This guiding mechanism presents an entirely new range of intriguing possibilities and is not achievable with conventional optical fibers. The concepts of band structure from solid-state physics are extended to electromagnetic waves in photonic crystal formations. Much like electrons are prohibited within the electrical band gap of semiconductors, light cannot propagate in a photonic band gap. A well-defined wavelength of light can be trapped and steered via a hollow fiber surrounded by a material with a photonic crystal structure by taking advantage of the photonic band gap confinement. Therefore, a higher refractive index of the center is not required<sup>13</sup>. In Fig. 4, a hollow core PCF of core diameter 'D', separation between the consecutive air holes (pitch) 'Λ' and air hole diameter 'd' is shown<sup>11</sup>.

## 4 Analysis of PCF Optical Properties

Following characteristics of PCFs are covered in this article birefringence, chromatic dispersion, confinement loss, effective mode area, nonlinearity, and zero dispersion wavelengths

### 4.1 Birefringence

In birefringent fibers, two orthogonally polarized modes travel at different speed in a single-mode

fiber. If the fiber causes the two-polarization mode to travel at different speed we say that this fiber has birefringence. Birefringence is a property of material in certain optical fiber where refractive index of the material changes with polarization state of the input light. There are many things in the fiber which causes birefringence, such as core stress, cladding eccentricity, elliptical fiber design, fiber twist, fiber stress and fiber bend etc. Due to birefringence in the fiber the two-polarization component travel at different speed and causes pulse broadening which is significant at high speed transmission.

Birefringence is an important optical property in fiber optics and many detecting devices because light needs to hold a straight polarization area, regularly requiring high birefringence. This optical phenomenon is typically observed in materials with uniaxial anisotropy, where the axis of symmetry is referred to as the optical axis of a particular material and there is no equivalent axis in the plane opposite to it<sup>14</sup>. Linear polarized light beam in parallel and opposite direction will have different effective refractive indices  $n_e$  and  $n_o$  for extra-ordinary and ordinary propagating beams separately. At the point when an un-captivated light emission goes through material with a nonzero intense edge to the optical axis, the oppositely spellbound segment may confront refraction at an edge according to the ordinary law of refraction and its contrary part a non-standard point appeared by the distinction between the two compelling refractive records called as the birefringence extent<sup>15</sup>.

$$\Delta n = n_e - n_o \quad \dots(1)$$

The difference between the real part values of the effective indices of the noticeable core own modes along with x-axis and y-axis- LP0<sub>1x</sub> and LP0<sub>1y</sub>.

$$B = \left| \text{Re}(n_{x,eff}) - \text{Re}(n_{y,eff}) \right| \quad \dots(2)$$

### 4.2 Chromatic Dispersion

The chromatic dispersion is the sum of the waveguide and material dispersions. Waveguide dispersion is caused by the structures of the fiber itself. Although the waveguide dispersion can be adjusted by varying the waveguide's parameter. The effective refractive index for any particular mode varies with wavelength for a fixed film thickness. The material dispersion is a hallmark of the material used to construct the fiber. In single mode fibers

material dispersion is more prominent than other types of dispersions. Dispersion is undesirable as it limits the bandwidth of the fiber. When nm ( $\lambda$ ) wavelength stabilizes and the true portion of the effective refractive index ( $n_{eff}$ ) comprises the scattering data, the material dispersion can be disregarded<sup>9</sup>.

$$D = -\frac{\lambda}{c} \frac{d^2 \text{Re}(n_{y,eff})}{d\lambda^2} \quad \dots(3)$$

Where  $\lambda$  is the operating wavelength and  $c$  is the velocity of light in vacuum.

#### 4.3 Confinement Loss

The presence of finite air holes in the core region guide the optical mode to leak from the inner core region to the outer air holes, which is unavoidable, resulting in confinement losses. The fundamental mode is used to determine confinement loss from the imaginary part of the complex effective index ( $n_{eff}$ ), utilizing

$$L_c = \frac{40\pi}{\ln(10)\lambda} \text{Im}(n_{eff}) \quad \dots(4)$$

The transfer of light from the core material to the exterior region is known as confinement loss. It can be adjusted based on variables such as pitch, air hole diameter, number of layers, and number of air holes<sup>15</sup>.

#### 4.4 Effective Mode Area

The following formulae yield the PCF's effective mode area, or  $A_{eff}$ :

$$A_{eff} = \frac{\left(\iint |E|^2 dx dy\right)^2}{\iint |E|^4 dx dy} \quad \dots(5)$$

One notable aspect of a tiny effective mode area is that, the optical intensities for a given power level are high, making nonlinearities essential<sup>16</sup>. Since  $E$  is the electric field amplitude, the integration is cross over the centre zone, yet over the full plane surface.

#### 4.5 Non-linearity

Non-linear The non-linear coefficient of PCF is an extremely important parameter in super continuum generation (SCG) analysis. Its nonlinear coefficient ( $\gamma$ ) is directly proportional to the effective area ( $A_{eff}$ ) and directly correlated to the nonlinear refractive index ( $n_2$ )<sup>16</sup>. The following equations represent the non-linear coefficient of PCF:

$$\gamma = \frac{2\pi n_2}{\lambda A_{eff}} \quad \dots(6)$$

#### 4.6 Supercontinuum generation

Laser pulses propagating in a nonlinear medium experience a large spectrum broadening due to a complex physical phenomenon called super continuum generation (SCG). SCG in optical fibers is a good source for many applications, including optical coherence tomography (OCT), ultrashort pulse compression, spectroscopy of materials and photonic structure, frequency metrology, fs-pulse phase stabilization, and fiber characterization, because of its spatial brightness and coherently pulsed nature<sup>17</sup>.

#### 5 Fabrication Techniques and Experimental Setup

A number of cutting-edge techniques are needed to improve the production of Photonic Crystal Fiber (PCF) based sensors in order to raise their sensitivity, dependability, and performance. The main developments have been made in its fabrication process through the use of the extrusion and stack and draw methods. The Stack-and-Draw Method is a technique that facilitates accurate and exact control over the PCF's microstructure, allowing for the production of intricate designs<sup>18</sup>. The fiber structure is more uniform and consistent when it is created using the extrusion method, which is also utilized to create fibers with complex patterns<sup>18</sup>. The performance of the sensor is significantly influenced by the material, in addition to the production method.

By strengthening the contact between the light and the analyte, doping with nanomaterials—adding metal nanoparticles, nanowires, or thin films—into the PCF structure can greatly increase sensor sensitivity<sup>19</sup>. The mechanical strength and flexibility of the fibers can be increased by using hybrid architectures, which combine various components—silica with polymers or other transparent materials. By more successfully containing light inside the core, hollow-core designs decrease light loss and increase sensitivity<sup>20</sup>. Higher sensitivity and reduced confinement losses are achieved by creative designs that make use of Rotated-Hexa and Hexagonal Core Structures to improve the field interaction with the analyte<sup>18</sup>. Improved selectivity and sensitivity for identifying specific analytes can be achieved by applying specialized coatings to the fiber surface during Surface Functionalization<sup>21</sup>.

The plasmonic effects can be amplified by coating the fiber with metals such as silver or gold, which will

further improve sensor performance<sup>19</sup>. The accuracy and resolution of the sensors can be improved by integrating PCFs with interferometric techniques<sup>19</sup>. Measurement reproducibility and reliability are increased when PCFs and microfluidic devices are combined because precise control over the sample environment is made possible<sup>22</sup>. These developments are opening the door for PCF-based sensors to become more effective and adaptable, which will make them appropriate for a variety of uses, including biomedical diagnostics and environmental monitoring.

The figures provide a brief summary of the experimental configurations frequently employed in PCF-based sensor research. A PCF-embedded chamber and a Light Source detection device comprise the experimental setup shown in Fig. 5. The light source is usually an LED or a laser. Spectrometers or photodetectors are used to examine the light that leaves the fiber. The presence of the target analyte is indicated by variations in the light's wavelength and intensity<sup>19</sup>. The application determines the different fiber designs. Hollow-core fibers and fibers with particular air-hole patterns are common designs<sup>23</sup>. The various experimental settings for sensing applications are shown in the figures below. The incident light is first fired from a light source with a wavelength ranging from 450 nm to 1600 nm.

Afterwards, a polarizer and polarizer-controller work together to transfer the light. The polarized light then travels through the sensor with the aid of a single-mode fiber (SMF-28). The light travels via single-mode fiber to an optical spectrum analyzer after passing through the sensor<sup>24</sup>. The sensor and SMF can now be properly coupled to a technique known as splicing. The SMF and PCF can be aligned using manual-mode translational and rotational alignment, and the splicing can be completed with a splicer that uses the filament fusion method<sup>25</sup>. An alternative splicing technique that joins the SMF and PCF is to insert an etched SMF tip into the PCF; coupling efficiency of 84.5% has been recorded for this procedure<sup>26</sup>. Additionally, a number of high-efficiency SMF-PCF couplers have been described by researchers<sup>27, 28</sup> that can also be utilized for this purpose.

An SMF with a coupling efficiency range of 80–90% can be coupled to a sensor. An analyte channel is implanted at an appropriate location to facilitate the liquid analyte entry and exit, as seen in

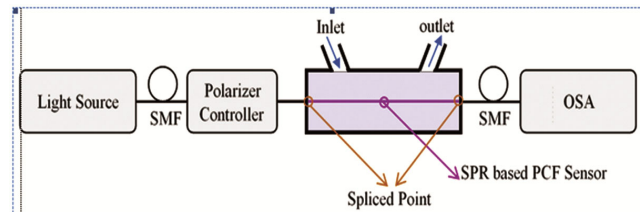


Fig. 5 — Experimental setup schematic of the proffered sensor for practical sensing applications

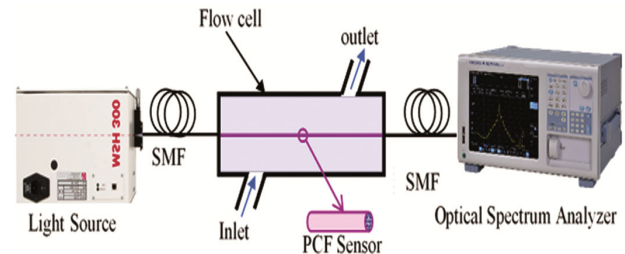


Fig. 6 — Experimental setup of the SPR sensor for refractive index (RI) detection<sup>34</sup>

Fig. 5. A tiny injection pumper that may be programmed is used to inject the analyte into the channel<sup>24</sup>.

Figure 6 displays the PCF-SPR sensor's schematic diagram. The interior surface of the grooves is covered with the gold film, which functions as a plasmonic material. These grooves have the advantages of quick analyte replacement and good accessibility, which makes them especially beneficial for metal painting. Femtosecond laser micromachining<sup>29</sup>, focused ion-beam milling<sup>30, 31</sup>, or chemical etching of the original side-hole PCF<sup>32, 33</sup> can all be employed to create the unique structure.

The schematic architecture of the suggested PCF-based SPR sensor for the glucose sensing application is shown in Fig. 7. In order to couple light into the PCF stub, the light source must be linked via a standard single mode (SMF) fiber. In order to link light into the spectrum analyzer and detect spectral changes throughout the process of sensing the glucose content of urine, a second SMF attached at the opposite end of the PCF was required. An optical-to-electrical (O/E) converter should be used to transform the optical signal from the second SMF into an electrical signal so that data may be analyzed.

A sensing application experimental setup is shown in Fig. 8. The test samples in the detecting zone regulate the light as it enters the PCF SPR sensor through the SMF. The signal processing unit is in charge of the regulated light. Following a procedure of normalization, the SPR spectrum is obtained.

### 6 Sensing Application of PCF

Unique properties are demonstrated by photonic crystal fibers in the field of sensing applications. Owing to the air holes positioned throughout the cladding region, these fibers possess an extraordinary ability to receive both gaseous and liquid samples. PCFs allow for the simultaneous use of fluid flow channels and light directing, which greatly enhances the interaction between light and samples.

#### 6.1 Liquid sensing application

Sensing in PCFs requires extremely small fluid volume samples, because of the laminate air holes and PCF core's tiny size. PCF requires a sample volume of 100 nanolitre to 10 microliters, while traditional optical fiber measuring techniques call for 1 to 10 millilitres. Applications in chemistry and biology, including the identification of hazardous chemicals,

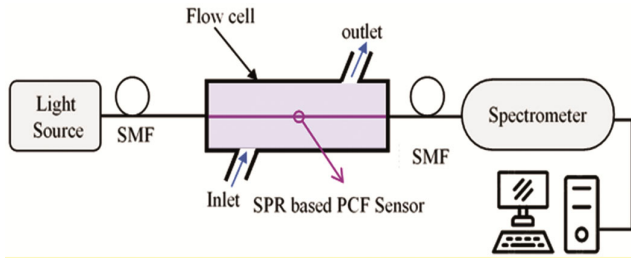


Fig. 7 — Schematic diagram of the PCF-based SPR sensor for sensing glucose level of urine<sup>35</sup>

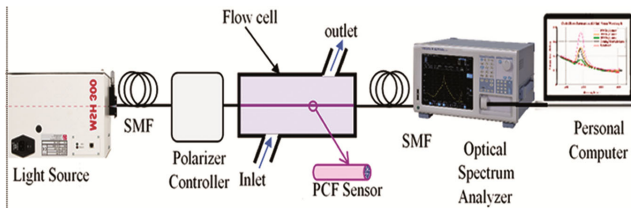


Fig. 8 — Schematic diagram of experimental setup of the PCF based sensor<sup>36</sup>

antibodies, blood components, cells, bacteria, DNA, and viruses, are highly interested in the incredibly small volume consumption.

The target materials in liquid sensing applications, such as water, ethanol, benzene, glucose, and human mucosa, fill the core pores. For liquid analytic detecting applications, PCF-based liquid sensors exhibit excellent sensitivity, high birefringence, and decreased confinement losses as shown in Table 1.

#### 6.2 Gas sensing application

Light propagation can be greatly controlled by adjusting the PCF structure (such as hexagonal, octagonal, and decagonal) and the core-cladding size with varied arrangements. The essential component for PCF-based sensors is evanescent field. PCF's light-controlling capabilities allows for intense customization of the evanescent field, which significantly enhances the performance of the gas sensor. Depending on the state, the gas exhibits varied features. Certain gases can be identified by PCF because they are particularly dangerous and flammable. Both residential areas and all industries may experience exploitation and fire due to the combustible gasses. Certain gases are poisonous and can lead to a variety of illnesses. A few gasses can also lead to other illnesses including cancer.

The matching gases' absorption lines are essential to the PCF-sensing system. The core region's modal intensities are displayed by the linked gas's detectable effective refractive index. Table 2 lists gas species with line strength and absorption in the near-infrared region.

#### 6.3 Chemical sensing application in THz regime

Researchers are putting forward and creating a variety of sensors in order to meet societal demands. The use of various chemicals is expanding quickly in order to better meet our everyday demands. Some of

Table 1 — Comparison of performance by means of birefringence, loss of confinement and sensitivity value for water as a target material at fixed wavelength,  $\lambda = 1.3 \mu\text{m}$  for reported PCFs.

Structure of air holes in PCF core region	Birefringence For water	Sensitivity (%) For water	Material's used	Confinement loss (dB/m) For water	Ref
Single circular air hole with varied diameters	0.00085	6	Water, Ethanol, Benzene	$6 \times 10^{-1}$	[52]
V-PCF and H-PCF with Elliptical shape air holes	0.0027	21	Water, Ethanol, Benzene	$1.10 \times 10^{-1}$	[53]
Circular and elliptical air holes	0.0028	43.84	Water, Ethanol	$2.07 \times 10^{-6}$	[54]
Single elliptical shape air hole	0.0050	41.36	Only Water	$2.16552 \times 10^{-10}$	[55]
Many circular air holes with varied diameter	0.0027	44.45	Water, 10% glucose solution, Human mucosa	$6.54489 \times 10^{-4}$	[56]

Table 2 — Description and absorption wavelength for different gases are shown.

Gases	Descriptions	Line strength ( $\text{cm}^{-2} \text{atm}^{-1}$ )	Absorption wavelength ( $\mu\text{m}$ )
Acetylene ( $\text{C}_2\text{H}_2$ )	Extremely flammable	$\sim 20 \times 10^{-2}$	1.533
Hydrogen iodide (HI)	Highly toxic, colourless	$0.775 \times 10^{-2}$	1.541
Ammonia ( $\text{NH}_3$ )	Toxic, irritating and destructive to tissues	$0.925 \times 10^{-2}$	1.544
Carbon monoxide (CO)	Combustion product, toxic, colourless	$0.0575 \times 10^{-2}$	1.567
Carbon dioxide ( $\text{CO}_2$ )	Main greenhouse gas	$0.048 \times 10^{-2}$	1.573
Hydrogen sulfide ( $\text{H}_2\text{S}$ )	Toxic, colourless, flammable	$0.325 \times 10^{-2}$	1.578
Methane ( $\text{CH}_4$ )	Flammable, greenhouse gas	$1.5 \times 10^{-2}$	1.667, 1.33
Hydrogen fluoride (HF)	Toxic, colourless, extremely corrosive	$32.5 \times 10^{-2}$	1.330
Hydrogen bromide (HBr)	Highly toxic, colourless	$0.0525 \times 10^{-2}$	1.341
Nitrogen dioxide ( $\text{NO}_2$ )	Greenhouse gas	$0.125 \times 10^{-2}$	0.800
Oxygen ( $\text{O}_2$ )	Strong oxidizer, supports and vigorously accelerates combustion	$0.01911 \times 10^{-2}$	0.761

Table 3 — Detail comparisons of recently reported PCF for chemical sensing application

f (THz)	R (%)	L ( $\text{cm}^{-1}$ )	$\alpha_{\text{eff}}$ ( $\text{cm}^{-1}$ )	$A_{\text{eff}}$ ( $\mu\text{m}^2$ )	Ref
1.0	60.05	$1.43 \times 10^{-11}$	-	$1.60 \times 10^5$	[22]
1.2	64.00	$1.12 \times 10^{-11}$	$3.30 \times 10^{-2}$	$4.40 \times 10^5$	[39]
1.0	74.54	$7.72 \times 10^{-08}$	$1.68 \times 10^{-2}$	-	[40]
1.3	78.80	$2.19 \times 10^{-09}$	-	$8.70 \times 10^5$	[7]
1.0	96.25	$2.11 \times 10^{-14}$	$9.16 \times 10^{-4}$	$1.29 \times 10^6$	[41]

these substances are bad for our health. Since alcohol, or ethanol, is regarded as the primary material, it is a chemical that is widely employed for a variety of applications<sup>37</sup>. These two are considered the primary analytes since they are present in the majority of chemical solutions<sup>38</sup>. Compared to other sensors, THz sensing is more practical since it offers non-ionizing effects and a sharp spatial resolution. Table 3 Shows studies related to chemical sensing of reported PCF at THz region.

#### 6.4 Temperature sensing application

In all fields of technological endeavour, industrial development and maintenance, and medical solutions, temperature measurement is a fundamental physical parameter. One significant discovery that offered a workable substitute for electronic temperature sensors was the creation of fiber-optic temperature sensors. When it comes to situations where radio frequency and electromagnetic interference pose serious obstacles to the use of electronic sensors, fiber-based temperature sensors have a clear practical advantage. Chemical plants, aviation, the electronics industry, the military, the thermal environment, and many more disciplines can benefit from the use of PCF-based temperature sensors.

In order to measure temperature shift in the 20–100 °C sensing range, an interferometer based on a PCF tip ended with a solid silica sphere was reported<sup>42</sup> with a sensitivity on the order of 10 pm/°C. This sensor's main benefit is its small size. Experiment demonstrations of a micro-cavity-based PCF interferometer for temperature variations from 26 °C to 103 °C show a wavelength sensitivity of 12 pm/°C<sup>43</sup>. The length of the PCF and the various splicing factors can be changed to further increase the sensitivity of this system.

A comparatively recent SPR-based nematic liquid crystal (NLC) PCF for temperature sensing that couples the SP mode on the surface of the nanogold with the core-guided mode within the PCF core that has been infiltrated with NLC<sup>44</sup>. In contrast to metal nanorods, which have no effect on the homogeneity of the electric field across the NLC core, it has a temperature sensitivity of 10 nm/°C over a temperature range of 30–50 °C. A new temperature sensor based on asymmetry in a dual-elliptical core PCF (DECPCF) structure was introduced<sup>45</sup>. It has a detection range of 30–34 °C over a 1.41cm DECPCF length, and its enhanced sensitivity is 42.99 nm/°C. Performance parameters of PCF-based temperature sensors for different PCF designs are shown in Table 4.

#### 7. Conclusions and Future Directions

Initially, the fundamentals of photonic crystal fiber and its guiding processes were studied in this article. Additionally, we go into great detail about the many PCF-based gas, liquid, and chemical sensor types as well as how background materials and core-cladding affect sensing performance. Chemical and gas sensors are increasingly being used in industry. Furthermore,

Table 4 — Performance parameters of PCF-based temperature sensors for different PCF designs

Ref	PCF Design	Sensitivity range of temperature	Sensitivity
[46]	Solid Core PCF with a central air-hole	-80 to 90	-6.020nm/°C
[47]	SPR based PCF	20 to 90	-2.150nm/°C
[48]	PM-PCF	25 to 42	2.580nm/°C
[49]	Q-dot nano-coating based PCF	25 to 42	0.1451nm/°C
[50]	Tip sensor-based PCF	100 to 700	0.110nm/°C
[51]	Ethanol-filled PBG fibers	25.6 to 50	-292pm/°C

dangerous and hazardous substances and gasses can be detected. Toxic gasses and chemicals can be detected using optical sensors, more especially photonic crystal fiber-based sensors. While a large amount of computational work has been done on PCF-based gas/chemical/temperature sensing, relatively little work has been investigated experimentally. It will take further experimental research to put the PCF-based gas, liquid, and chemical sensors into practical use.

Photonic Crystal Fibers (PCFs) have emerged as a transformative technology in the realm of optical sensing, offering a range of advantages over traditional optical fibers. This review has highlighted the key advancements and applications of PCF-based sensors, revealing their significant impact and future potential. The advancements in PCF-based sensing technologies underscore their transformative potential across multiple domains. The high sensitivity and selectivity of PCF sensors provide new opportunities for precision measurements and monitoring, offering substantial benefits in fields such as healthcare, environmental science, and industrial processes.

Following future directions may be opted for the improvement of performance of the PCF based devices.

- The PCF structure must be made simpler in order to make fabrication easier. The core region is crucial for PCF-based gas/chemical/temperature sensors since gases and chemicals typically flow through it. To absorb the light as much as possible, a result must create a proper core structure.
- Controlling the propagation loss is necessary for the practical realization. If not, light will instantly disappear after being launched from one end of the fiber, making it impossible for it to produce a detectable signal at the other end.

- The majority of the documented PCF-based gas/chemical/temperature sensors require selective gas/chemical filtrations. This presents additional obstacle to practical implementation. An alternate remedy would be to use external chemical and/or gas monitoring techniques.
- The integration of PCF sensors with emerging technologies, such as IoT and machine learning, has opened new avenues for real-time data analysis and smart sensing solutions. This integration promises to enhance the utility of PCF sensors in various applications, providing more insightful and actionable data.

## References

- 1 Yang K-Y, Chau Y-F, Huang Y-W, Yeh H-Y & Tsai D P, *J Appl Phys*, 109 (2011).
- 2 Yakasai I, Abas P E, Kaijage S F, Caesarendra W & Begum F, *Photonics*, 6 (2019) 78.
- 3 Wang F, Sun Z, Liu C, Sun T & Chu P K, *Opto-Electron Rev*, 26 (2018) 50.
- 4 Gupta B D & Verma R K, *J Sensors*, 2009 (2009).
- 5 Otupiri R, Akowuah E K & Haxha S, *Optics Express*, 23 (2015) 15716.
- 6 Mishra S S & Singh V K, *J Microwaves, Optoelectron Electromagn Appl*, 10 (2011) 33.
- 7 Liu C, Yang L, Lu X, Liu Q, Wang F, Lv J, Sun T, Mu H & Chu P K, *Opt Exp*, 25 (2017) 14227.
- 8 Hasan M, Akter S, Rifat A, Rana S & Ali S, *Photonics*, 4 (2017) 18.
- 9 Xiao L, Demokan M S, Jin W, Wang Y & Zhao C-L, *J Lightwave Technol*, 25 (2007) 3563.
- 10 Wadsworth W J, Ortigosa-Blanch A, Knight J C, Birks T A, Man T-P M & Russell P S J, *J Opt Soc Am B*, 19 (2002) 2148.
- 11 Shashidharan S & Johny J, *2012 IV International Congress on Ultra Modern Telecommunications and Control Systems*, 2012.
- 12 Russell P & Dettmer R, *IEE Review*, 47 (2001) 19.
- 13 Rahaman M E, Jibon R H, Mondal H S, Hossain M B, Bulbul A A-M & Saha R, *Sens Bio-Sens Res*, 32 (2021) 100422.
- 14 Paul B K, Ahmed K, Vigneswaran D, Ahmed F, Roy S & Abbott D, *IEEE Sens J*, 18 (2018) 9948.
- 15 Mahnot N, Maheshwary S & Mehra R, *Photonic Crystal Fiber- An Overview*, 2015.
- 16 Knight J C, *Photonic crystal fibres*, *Nature*, 424 (2003) 847.
- 17 Kanmani R, Ahmed K, Roy S, Ahmed F, Paul B K & Rajan M S M, *Optik*, 194 (2019) 163084.
- 18 Hossain M S & Sen S, *Silicon*, 13 (2020) 3879.
- 19 Hu D J J, Wong R Y-N & Shum P P, *Photonic Crystal Fiber-Based Interferometric Sensors*, in *Selected Topics on Optical Fiber Technologies and Applications*, In Tech, 2018.
- 20 Jing J, Liu K, Jiang J, Xu T, Wang S, Ma J, Zhang Z, Zhang W & Liu T, *Photon Res*, 10 (2021) 126.
- 21 Shobug M A, Noor K S, Raj A G S, Ramkumar G, Padmanaban P, Mallan S, Ferdous A H M I, Bani M M & Rashed A N Z, *Fuel quality assurance based on hybrid*

- hexagonal circular hollow core PCF sensing through management of terahertz region operation, *J Opt*, (2024).
- 22 Ademgil H & Haxha S, *Sensors*, 15 (2015) 31833.
  - 23 Portosi V, Laneve D, Falconi M C & Prudenzano F, *Sensors*, 19 (2019) 1892.
  - 24 Liu Z, Wei Y, Zhang Y, Zhu Z, Zhao E, Zhang Y, Yang J, Liu C & Yuan L, *Opt Commun*, 366 (2016) 107.
  - 25 Jaroszewicz L R, Murawski M & Stasiewicz K, *Photon Lett Poland*, 1 (2009).
  - 26 Fan D, Jin Z, Wang G, Xu F, Lu Y, Hu D J J, Wei L, Shum P & Zhang X, *IEEE Photon J*, 9 (2017) 1.
  - 27 Wei H, Zhu Y & Krishnaswamy S, *IEEE Photon Technol Lett*, 27 (2015) 2142.
  - 28 Yokota H, Yashima H, Imai Y & Sasaki Y, *Adv Opto Electron*, 2016 (2016) 1.
  - 29 Brakel A van, Grivas C, Petrovich M N & Richardson D J, *Opt Exp*, 15 (2007) 8731.
  - 30 Wang F, Yuan W, Hansen O & Bang O, *Opt Exp*, 19 (2011) 17585.
  - 31 Martelli C, Olivero P, Canning J, Groothoff N, Gibson B & Huntington S, *Opt Lett*, 32 (2007) 1575.
  - 32 Frazão O, Martynkien T, Baptista J M, Santos J L, Urbanczyk W & Wojcik J, *Opt Lett*, 34 (2008) 76.
  - 33 Erdmanis M, Viegas D, Hautakorpi M, Novotny S, Santos J L & Ludvigsen H, *Opt Exp*, 19 (2011) 13980.
  - 34 Han H, Hou D, Zhao L, Luan N, Song L, Liu Z, Lian Y, Liu J & Hu Y, *Sensors*, 20 (2020) 1009.
  - 35 Rahaman M E, Jibon R H, Ahsan M S, Ahmed F & Sohn I-B, *Plasmonics*, 17 (2021) 1.
  - 36 Hossen M N, Ferdous M, Khalek M A, Chakma S, Paul B K & Ahmed K, *Sens Bio-Sens Res*, 21 (2018) 1.
  - 37 Arif M F H & Biddut M J H, *Optik*, 131 (2017) 697.
  - 38 Arif M F H, Hossain M M, Islam N & Khaled S M, *Sens Bio-Sens Res*, 22 (2019) 100252.
  - 39 Ademgil H & Haxha S, *Optik*, 127 (2016) 6653.
  - 40 2. COMSOL Multiphysics User's Guide.
  - 41 Iqbal F, Biswas S, Bulbul A A-M, Rahaman H, Hossain M B, Rahaman M E & Awal M A, *Sens Bio-Sens Res*, 30 (2020) 100384.
  - 42 Mileńko K, Hu D J J, Shum P P, Zhang T, Lim J L, Wang Y, Woliński T R, Wei H & Tong W, *Opt Lett*, 37 (2012) 1373.
  - 43 Dash J N & Jha R, *IEEE Photon Technol Lett*, 27 (2015) 1325.
  - 44 Hameed M F O, Azab M Y, Heikal A M, El-Hefnawy S M & Obayya S S A, *IEEE Photon Technol Lett*, 28 (2016) 59.
  - 45 Ayyanar N, Raja R V J, Vigneswaran D, Lakshmi B, Sumathi M & Porsezian K, *Opt Mater*, 64 (2017) 574.
  - 46 Ma J, Yu H H, Jiang X & Jiang D S, *Opt Exp*, 25 (2017) 9406.
  - 47 Liu Q, Li S, Chen H, Li J & Fan Z, *Appl Phys Exp*, 8 (2015) 046701.
  - 48 Cui Y, Shum P P, Hu D J J, Wang G, Humbert G & Dinh X-Q, *IEEE Photon J*, 4 (2012) 1801.
  - 49 Larrión B, Hernández M, Arregui F J, Goicoechea J, Bravo J & Matías I R, *J Sensors*, 2009 (2009).
  - 50 Park B, Provine J, Jung I W, Howe R T & Solgaard O, *IEEE Sens J*, 11 (2011) 2643.
  - 51 Dong B, Shen Z, Yu C & Wang Y, *J Lightwave Technol*, 34 (2016) 3853.
  - 52 Hasan M M, Sen S, Rana M J, Paul B K, Habib M A, Daiyan G M & Ahmed K, "Heptagonal Photonic Crystal Fiber Based Chemical Sensor in THz Regime," in *2019 Joint 8th International Conference on Informatics, Electronics & Vision (ICIEV) and 2019 3rd International Conference on Imaging, Vision & Pattern Recognition (icIVPR)*, 2019.
  - 53 Chen M-Y, Yu R-J & Zhao A-P, *J Lightwave Technol*, 23 (2005) 2707.
  - 54 Chaudhary L, *Int J Res Appl Sci Eng Technol*, 5 (2017) 1828.
  - 55 Buczynski R, *Acta Physica Polonica A*, 106 (2004) 141.
  - 56 Leon M J B M, Abedin S & Kabir M A, *Sens Int*, 2 (2021) 100061.